

EVIDENCE FOR A PRE-ERUPTIVE TWISTED FLUX ROPE USING THE THEMIS VECTOR MAGNETOGRAPH

A. CANOU¹, T. AMARI^{1,5}, V. BOMMIER², B. SCHMIEDER³, G. AULANIER³, AND H. LI⁴

¹ CNRS, Centre de Physique Théorique de l’Ecole Polytechnique, F-91128 Palaiseau Cedex, France; amari@cph.polytechnique.fr

² Observatoire de Paris, LERMA, 5 place Jules Janssen, F-92190 Meudon cedex, France

³ Observatoire de Paris, LESIA, 5 place Jules Janssen, F-92190 Meudon cedex, France

⁴ Purple Mountain Observatory, Nanjing 210008, People’s Republic of China

Received 2008 December 15; accepted 2009 January 13; published 2009 February 11

ABSTRACT

Although there is evidence that twisted structures form during large-scale eruptive events, it is not yet clear whether these exist in the pre-eruptive phase as twisted flux ropes (TFRs) in equilibrium. This question has become a major issue since several theoretical mechanisms can lead to the formation of TFRs. These models consider either the evolution of a coronal configuration driven by photospheric changes or the emergence of TFR from the convection zone. We consider as a target for addressing this issue the active region NOAA AR 10808 known at the origin of several large-scale eruptive phenomena, and associated with the emergence of a δ -spot. Using the THEMIS vector magnetogram as photospheric boundary conditions for our nonlinear force-free reconstruction model of the low corona and without any other assumption, we show that the resulting pre-eruptive configuration exhibits a TFR above the neutral line of the emerging δ -spot. In addition, the free magnetic energy of this configuration could even be large enough to explain such resulting large-scale eruptive events.

Key words: MHD – Sun: corona – Sun: magnetic fields

1. INTRODUCTION

A typical coronal mass ejection (CME) structure contains a front, a dark cavity, and a plasmoid. This plasmoid has often been associated with the cool material of a prominence which is ejected with the CME, with a typical mass of 10^{16} g and an average speed of 10^3 km s⁻¹ (see Gopalswamy et al. (2006) and Forbes et al. (2006), for interesting reviews of the many observations relevant to the CME model and constraints). A key issue is whether this prominence is just tracing the visible CME phenomenon as a passive entity, or if it plays an active role in the initiation of the mechanism itself.

Observations show the presence of twist in the eruptive prominence (as in the well known “Granddaddy” prominence). Gary & Moore (2004) made a quantitative study showing that during the eruptive phase a twisted structure clearly appears in favor of a twisted flux rope (TFR; Gibson et al. 2006). However, this does not represent evidence for the existence of this twisted structure prior to the eruption. Therefore, determining the nature of the pre-eruptive configuration is an important issue.

Although it is now well known that the magnetic field is dominant in the low corona, it is not yet fully accessible in the corona by observational means. A large variety of models have been proposed for the pre-eruptive magnetic configuration; these can be gathered into two generic classes: the TFR model and the magnetic arcade one. These are intimately related to the determination of the magnetic structure responsible for the support of prominence in their magnetic dips (Forbes et al. 2006; Dudík et al. 2008). Both these types of pre-eruptive configuration models have also been shown to lead to large-scale disruptions, either in simple topology (such as the flux cancellation model; Amari et al. 2000) or in complex topology only (such as the breakout model (Antiochos et al. 1999) or also the flux cancellation model (Amari et al. 2007)).

On the other hand, assuming the presence of a TFR in the convection zone (CZ), numerical simulations of emerging TFR

have been given a great deal of attention to attempt to deduce both emergence through the CZ and across the photosphere (Fan 2001; Magara & Longcope 2003; Archontis et al. 2004; Galsgaard et al. 2005; Manchester et al. 2004; Cheung et al. 2007).

However, without any assumption in the above coronal models proposed for the formation of a TFR or without assuming the pre-existence of such TFR in the CZ, it has not yet been proven that such TFRs exist in the corona after emergence of subphotospheric structures.

For this reason, solar physicists have turned toward the determination of the three-dimensional coronal configuration, using boundary conditions from various photospheric magnetograms of ground-based (IVM, SOLIS, ASP, and THEMIS) or embarked (*Hinode*, *SDO* in the future) vector magnetographs. This problem has been called the *reconstruction problem*. Although solving this problem is still an active field of research (Amari et al. 1997; Schrijver et al. 2006; Aly & Amari 2007; Wiegmann 2008), there exist few cases for which TFRs have been successfully reconstructed in the pre-eruptive configuration (Régnier & Amari 2004), although this case does not correspond to the case of an emerging active region (AR).

Qualitative arguments of association of an emerging AR and the apparition of a TFR in the corona have been shown (Lites & Low 1997). An emerging delta-type sunspot (δ -spot) in active region NOAA AR 10808 exhibiting tongues gives indications that a TFR is emerging from below (López Fuentes et al. 2000). What is the coronal signature of this emerging structure? Is there quantitative evidence of a TFR present in the corona?

In this Letter, we report a contribution to the solution of that problem. This AR has been observed by THEMIS, thus providing a vector magnetogram. Using these data without any other assumption but that the low corona is force free, we reconstruct the coronal magnetic field as a nonlinear force-free (NLFF) field using our reconstruction code XTRAPOL (Amari et al. 2006). We thus determine the nature of the pre-eruptive configuration, and in particular above the emerging δ -spot.

⁵ Associate scientist at Observatoire de Paris, LESIA, 5 place Jules Janssen, F-92190 Meudon cedex, France.

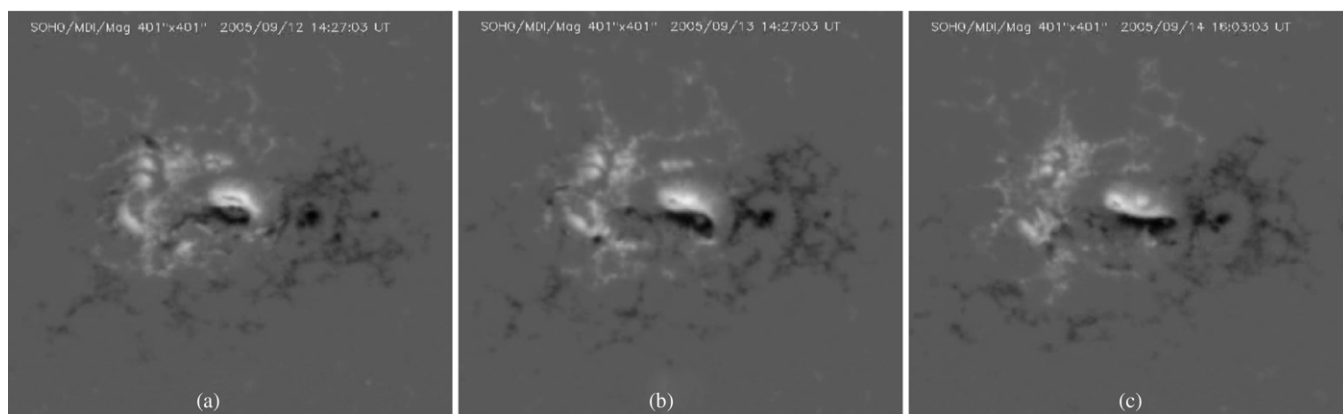


Figure 1. *SOHO*/MDI magnetogram during the emergence of the δ -spot from 2005 September 12 to September 14. One clearly sees evidence of tongue formation on panels (a), (b), and (c).

2. ACTIVE REGION AR 10808 AND RECONSTRUCTION MODEL

On 2005 September 7, NOAA AR 10808 appeared on the east limb of the solar disk in the Southern Hemisphere. It was a very flare-productive AR: during its appearance more than 10 X-class and 25 M-class flares occurred. In panel (b) of the *Solar and Heliospheric Observatory (SOHO)*/MDI magnetogram (see Figure 1), we see that AR 10808 is composed of an emerging δ -spot with two elongated tongues surrounded by two opposite diffuse polarities. The δ -spot underwent a counterclockwise rotation motion of its two polarities, such that their orientation is in agreement with Hale's law (Hale et al. 1919). The two more diffuse opposite polarities that surround the δ -spot also satisfy Hale's law and are the remaining polarities of the older AR 10798.

We base our study on the data obtained by the ground-based THEMIS telescope located on Tenerife. The AR was observed from 14:25 UT to 15:25 UT on 2005 September 13 before an X1.5 flare which lead to the eruption of a large filament and an X1.7 flare which lead to a CME (see, respectively, Nagashima et al. (2007) and Li et al. (2007b) for detailed studies of these events). THEMIS was in the MTR mode using the Fe I 6302.5 Å line (see López Ariste et al. (2000) for a detailed description of the THEMIS instrumentation). The MTR observing mode allows polarimetric observations with a spatial resolution of $0''.4 \text{ pixel}^{-1}$. After correcting the dark current and flat field, one can extract the four Stokes parameters and then, using the UNNOFIT inversion code (Bommier et al. 2007), the three components of the magnetic field are derived. The 180° ambiguity was solved using the method of Wang et al. (2001). So we finally have the three components $B_{x,\text{phot}}$, $B_{y,\text{phot}}$, and $B_{z,\text{phot}}$ of the solar magnetic field expressed in the Sun's Cartesian frame.

In Figure 2(a), the THEMIS vector magnetogram with the ambiguity solved is shown. One can note that some vectors point from the negative to the positive polarity (the circles in Figure 2(a)). This is a feature of an inverse configuration (Li et al. 2007a) and may represent an indication for the presence of a TFR. Furthermore, on the west part of the δ -spot the tangential component exhibits a normal configuration which is proper to sheared arcades. The presence of tongues and the inverse configuration are both evidence for the emergence of a TFR (López Fuentes et al. 2000).

One assumes that the domain is filled up with a zero- β plasma, thus assumed to be in a force-free state, which

represents a reasonable approximation for the low- β corona. The magnetic field above the AR is then reconstructed using the code XTRAPOL (Amari et al. 1997, 2006). Based on the Grad–Rubin algorithm (Grad & Rubin 1958), it solves the set of NLFF equations as a well posed problem. These equations are not reproduced here.

This set of equations needs α_{phot} and $B_{z,\text{phot}}$ as boundary conditions. These are directly computed from the vector magnetogram: $B_{z,\text{phot}}$ is the z -component of the magnetic field whereas, adopting the same strategy as in Régnier & Amari (2004), α_{phot} is defined as $\alpha_{\text{phot}} = \frac{j_{z,\text{phot}}}{B_{z,\text{phot}}}$, where $j_{z,\text{phot}}$ is the vertical current density.

Given the way α_{phot} is computed and since $B_{z,\text{phot}}$ becomes small near the polarity inversion line (PIL), we have to impose a threshold on $|B_{z,\text{phot}}|$ under which we set α_{phot} to zero. Moreover, the computation of $j_{z,\text{phot}}$ implies a discrete derivative of the tangential components. In order to avoid its unreliable values due to sudden variations of $B_{x,\text{phot}}$ or $B_{y,\text{phot}}$ below the noise level, we also fix a threshold on the norm of the tangential component $\|\mathbf{B}_t\|$ below which we set $j_{z,\text{phot}}$ to zero. α_{phot} is then smoothed and interpolated on the computational mesh. The result of the processing is shown in Figure 2(b) and one can note that the inverse configuration is not damaged during this step (see the circles).

It is to noted that, because of magnetic flux imbalance in the lower boundary, we use open boundary conditions for XTRAPOL. That is, the field lines are allowed to reach lateral and top boundaries in such a way that the flux is balanced for the six boundaries of our simulation domain.

3. RESULTS AND DISCUSSION

Using the values of $B_{z,\text{phot}}$ and α_{phot} as boundary conditions for our reconstruction model, we compute the magnetic field in a computational domain of size $[-69; 69] \times [-35; 35] \times [0; 143] \text{ Mm}^3$ discretized on a nonuniform mesh with $158 \times 125 \times 120$ grid points. We use a cutoff value of 40 G for both $\|\mathbf{B}_t\|$ and $|B_{z,\text{phot}}|$.

The following features are observed in the computed configuration.

1. In Figure 3, the selected field lines have been drawn. The configuration reveals an emerged TFR only along the east part of the δ -spot PIL with the presence of bald patches below. This is in agreement with the presence of the inverse configuration. It presents a twist of 2π , an altitude of

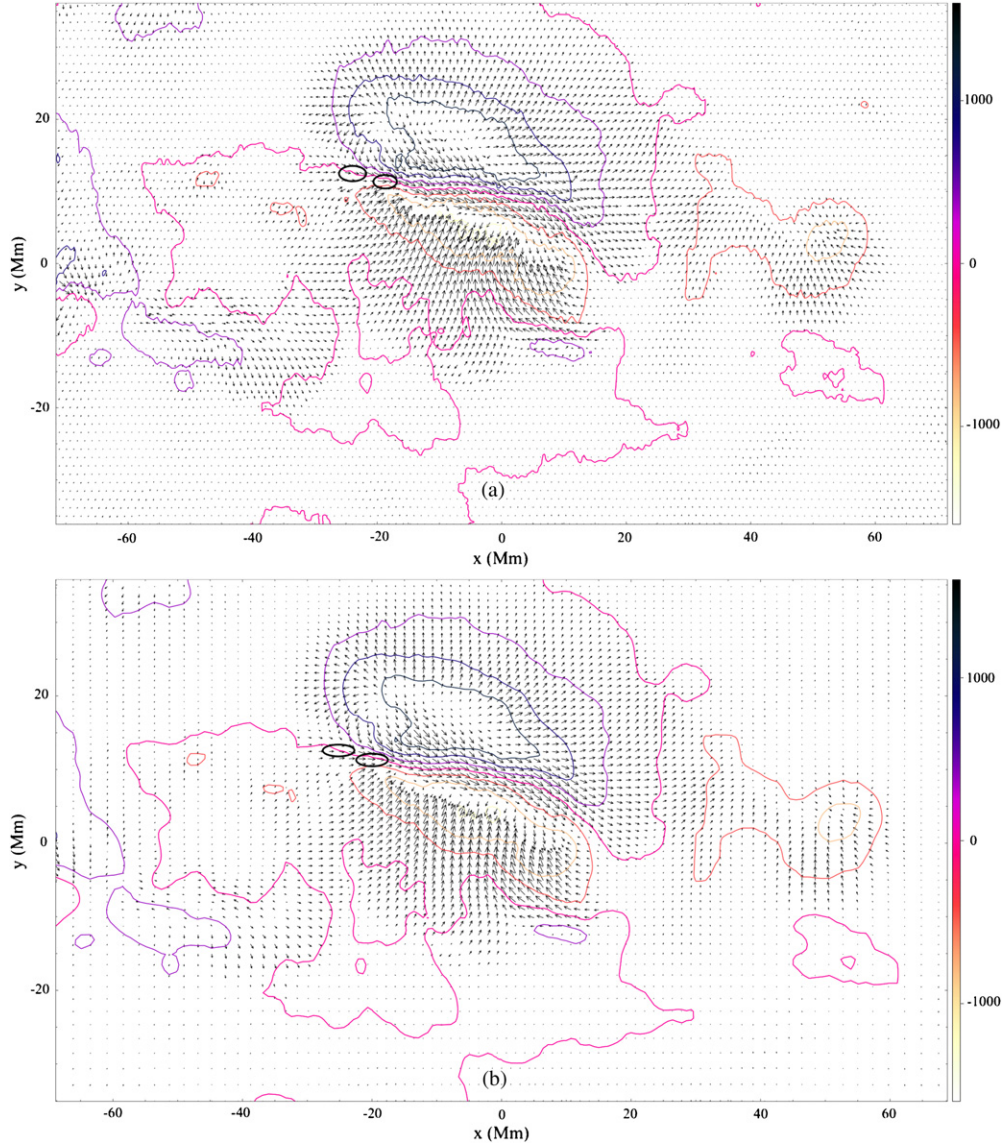


Figure 2. Transverse magnetic field measured by THEMIS on 2005 September 13 at 15:25 UT: (a) original data and (b) processed data. The overlaid contour levels of the normal magnetic field are 0, ± 400 , ± 800 , and ± 1200 G.

1.72 Mm, and a length of 23.96 Mm. The value of α lies between 1.22 and 1.88 Mm^{-1} and the current density is about 26.2 mA m^{-2} and -60.5 mA m^{-2} in the positive and negative polarities, respectively. One can note that, on the one hand, the TFR is overlaid by a strongly sheared magnetic field and that, on the other hand, sheared arcades are present on the west part of the δ -spot, as guessed from Figure 2.

- Using the same notations as in Amari et al. (2003), the magnetic energy is defined as $W[\mathbf{B}] = \int_{\Omega} \frac{B^2}{2\mu_0} dV$. However, it is more relevant to compute the free magnetic energy defined as $\Delta W = W[\mathbf{B}] - W_{\pi}$, where $W[\mathbf{B}]$ and W_{π} are the energies of the NLFF and potential configurations, respectively. The free energy represents the maximum energy that can be released during a CME. Thus, $W_{\pi} = 3.31 \times 10^{32}$ erg, $W[\mathbf{B}] = 4.88 \times 10^{32}$ erg, and $\Delta W = 1.57 \times 10^{32}$ erg. For this flux distribution, the open-field energy is $W_{\sigma} = 2.18 W_{\pi}$, whereas $W[\mathbf{B}] = 1.47 W_{\pi}$; this clearly satisfies $W_{\pi} \leq W[\mathbf{B}] < W_{\sigma}$ (Aly 1991). So the maximum energy that can be released during the flare is 47% of that of the potential field. This value is similar to that of a large flare, that

is 3×10^{32} erg (Priest & Forbes 2002). On the one hand, this value is similar to that found by Régnier & Amari (2004), who found a TFR, and to that of Thalmann & Wiegmann (2008), who studied a flare-productive AR. On the other hand, this ratio is much greater than that computed in Thalmann et al. (2008) and Guo et al. (2008) where no TFR was found. Thus, such large free magnetic energy might be able to explain why AR 10808 suffers two major disruptions in few hours.

- The total relative magnetic helicity ΔH_m can easily be computed from our model which solves the vector potential \mathbf{A} with our gauge choice using the formula of Finn & Antonsen (1985), $\Delta H_m = \int_{\Omega} (\mathbf{A} + \mathbf{A}_{\pi}) \cdot (\mathbf{B} - \mathbf{B}_{\pi}) dV$. One gets $\Delta H_m = 6.07 \times 10^{42} \text{ G}^2 \text{ cm}^4$. This value is positive, as is the mean value of α , which is in agreement with the chirality rules for an AR located in the Southern Hemisphere. This value can be compared to those computed in Bleybel et al. (2002) and Régnier & Amari (2004) which also found twisted magnetic structures. However, since there is no upper bound as for the magnetic energy, this value cannot

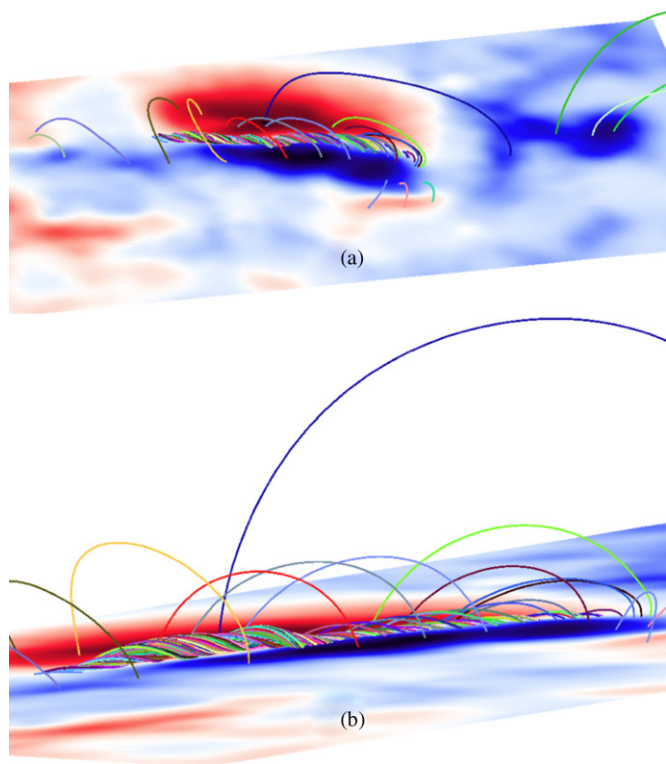


Figure 3. Set of field lines reconstructed with the code XTRAPOL as an NLFF field using the THEMIS vector magnetogram as boundary data. It shows the presence of a TFR in equilibrium above the emerging δ -spot.

be relevant to compare to any critical value. This value does not give the amount of self-magnetic helicity “stored” in the TFR, which might not be negligible. However, defining and computing partial magnetic helicity, which would require a partitioning of the domain, is not an easy task to do in a meaningful way.

In conclusion, the data provided by THEMIS allowed us to highlight the presence of a TFR located above the emerging δ -spot in AR 10808. This result may represent the first case of quantitative evidence of existence of a TFR in the corona associated with an emerging pair of spots. Since the presence of tongues observed in the structure represents evidence for the emergence of a TFR, our results build a bridge between the underlying TFR structure and the coronal configuration which is also a TFR. Moreover, since TFRs have been shown to be good candidates for explaining large-scale eruptive events in the context of magnetohydrodynamic (MHD) mechanisms (see Amari & Aly 2009), our results show that because of the large amount of free magnetic energy available in the reconstructed configuration the presence of the TFR may be an important ingredient at the origin of the eruptive events which occurred in AR 10808.

However, we do not pretend that this is the only possible type of configuration which may lead to an eruption in general.

A more extended study including the effect on the model of various methods for solving the 180° ambiguity as well as data provided by various vector magnetographs, and the physics of the AR will be presented in a forthcoming paper (A. Canou et al. 2009, in preparation).

We thank N.-E. Raouafi for his diagnostic of the magnetograms.

REFERENCES

- Aly, J. J. 1991, *ApJ*, **375**, L61
- Aly, J. J., & Amari, T. 2007, *Geophys. Astrophys. Fluid Dyn.*, **101**, 249
- Amari, T., & Aly, J. J. 2009, in Proc. IAU Symp. 257, Universal Heliospherical Processes, ed. N. Gopalswamy & D. F. Webb (Cambridge: Cambridge Univ. Press)
- Amari, T., Aly, J. J., Luciani, J. F., Boulmezaoud, T. Z., & Mikic, Z. 1997, *Sol. Phys.*, **174**, 129
- Amari, T., Aly, J. J., Mikic, Z., & Linker, J. 2007, *ApJ*, **671**, L189
- Amari, T., Boulmezaoud, T. Z., & Aly, J. J. 2006, *A&A*, **446**, 691
- Amari, T., Luciani, J. F., Aly, J. J., Mikic, Z., & Linker, J. 2003, *ApJ*, **585**, 1073
- Amari, T., Luciani, J. F., Mikic, Z., & Linker, J. 2000, *ApJ*, **529**, L49
- Antiochos, S. K., DeVore, C. R., & Klimchuk, J. A. 1999, *ApJ*, **510**, 485
- Archontis, V., Moreno Insertis, F., Galsgaard, K., Hood, A., & O’Shea, E. 2004, *A&A*, **426**, 1047
- Bleybel, A., Amari, T., van Driel-Gesztelyi, L., & Leka, K. D. 2002, *A&A*, **395**, 685
- Bommier, V., Landi Degl’Innocenti, E., Landolfi, M., & Molodij, G. 2007, *A&A*, **464**, 323
- Cheung, M. C. M., Schüssler, M., & Moreno Insertis, F. 2007, *A&A*, **467**, 703
- Dudík, J., Aulanier, G., Schmieder, B., Bommier, V., & Roudier, T. 2008, *Sol. Phys.*, **248**, 29
- Fan, Y. 2001, *ApJ*, **554**, L111
- Finn, J. M., & Antonsen, T. M. 1985, *Comm. Plasma Phys. Control. Fusion*, **9**, 111
- Forbes, T. G., et al. 2006, *Space Sci. Rev.*, **123**, 251
- Galsgaard, K., Moreno Insertis, F., Archontis, V., & Hood, A. 2005, *ApJL*, **618**, L153
- Gary, G. A., & Moore, R. L. 2004, *ApJ*, **611**, 545
- Gibson, S. E., Fan, Y., Török, T., & Kliem, B. 2006, *Space Sci. Rev.*, **124**, 131
- Gopalswamy, N., Mikić, Z., Maia, D., Alexander, D., Cremades, H., Kaufmann, P., Tripathi, D., & Wang, Y.-M. 2006, *Space Sci. Rev.*, **123**, 303
- Grad, H., & Rubin, H. 1958, Proc. 2nd Int. Conf. on Peaceful Uses of Atomic Energy, Vol. 31 (Geneva: United Nations), 190
- Guo, Y., Ding, M. D., Wiegmann, T., & Li, H. 2008, *ApJ*, **679**, 1629
- Hale, G. E., Helderman, F., Nicholson, S. B., & Joy, A. H. 1919, *ApJ*, **49**, 153
- Li, J., Amari, T., & Fan, Y. 2007a, *ApJ*, **654**, 675
- Li, H., Schmieder, B., Song, M. T., & Bommier, V. 2007b, *A&A*, **475**, 1081
- Lites, B. W., & Low, B. C. 1997, *Sol. Phys.*, **174**, 91
- López Ariste, A., Rayrole, J., & Semel, M. 2000, *A&AS*, **142**, 137
- López Fuentes, M. C., Demoulin, P., Mandrini, C. H., & van Driel-Gesztelyi, L. 2000, *ApJ*, **544**, 540
- Magara, T., & Longcope, D. W. 2003, *ApJ*, **586**, 630
- Manchester IV, W., Gombosi, T., DeZeeuw, D., & Fan, Y. 2004, *ApJ*, **610**, 161
- Nagashima, K., Isobe, H., Yokoyama, T., Ishii, T. T., Okamoto, T. J., & Shibata, K. 2007, *ApJ*, **668**, 533
- Priest, E. R., & Forbes, T. G. 2002, *A&AR*, **10**, 313
- Régnier, S., & Amari, T. 2004, *A&A*, **425**, 345
- Schrijver, C. J., et al. 2006, *Sol. Phys.*, **235**, 161
- Thalmann, J. K., & Wiegmann, T. 2008, *A&A*, **484**, 495
- Thalmann, J. K., Wiegmann, T., & Raouafi, N.-E. 2008, *A&A*, **488**, L71
- Wang, H., Yan, Y., & Sakurai, T. 2001, *Sol. Phys.*, **201**, 323
- Wiegmann, T. 2008, *J. Geophys. Res. (Space Phys.)*, **113**, 3